Diagnostic and Interventional Imaging 103 (2022) 266–272

Original article/*Abdominal imaging*

Accuracy of a CT density threshold enhancement to identify pancreatic parenchyma necrosis in acute pancreatitis during the first week

Jean Pierre Tasu[a,b,*], Raphael Le Guen[a], Inès Ben Rhouma[a], Ayoub Guerrab[a], Nadeem Beydoun[a], Brice Bergougnoux[a], Pierre Ingrand[c], Guillaume Herpe[a]

[a] *Department of Diagnostic and Interventional Radiology, University Hospital of Poitiers, 86021 Poitiers, France*
[b] *LaTim, UBO and INSERM 1101, University of Brest, 29000 Brest, France*
[c] *CIC 1402, Clinical Investigation center, Bio-statistic and epidemiology, University of Poitiers, 86021 Poitiers, France*

ARTICLE INFO

Keywords:
Acute necrotizing pancreatitis
Multidetector row CT (MDCT)
X-ray computed tomography
Threshold CT value
Revised Atlanta Classification

ABSTRACT

Purpose: The purpose of this study was to identify attenuation threshold value on computed tomography (CT) that allowed discriminating between interstitial edematous pancreatitis (IEP) and necrotizing pancreatitis (NP) in patients with acute pancreatitis during the first week of the disease and evaluate interobserver reproducibility for the diagnosis of acute pancreatitis category.

Materials and methods: Patients with acute pancreatitis who underwent CT examination of the abdomen between March 2015 and December 2019 were retrospectively included. Actual diagnosis of IEP or NP was based on final clinical report, follow-up evaluation, and complications. Six regions of interest were manually placed in the pancreatic gland and peripancreatic fat, and differences in CT attenuation values before contrast injection and during the portal venous phase of enhancement were computed. Performance in the diagnosis of AP category was evaluated using receiver operating characteristic analysis. Interobserver agreement was estimated by the intraclass correlation coefficient (ICC) and Bland Altman analysis was used to estimate reproducibility between pairs of observers.

Results: Sixty-six patients with NP (46 men, 20 women; mean age, 55 ± 17 [SD] years; age range: 20-89 years) and 70 patients with IEP (39 men, 31 women; mean age, 54 ± 18 [SD] years; age range: 21–87 years) were included. An enhancement value less than 30 Hounsfield units (HU) in the pancreatic gland during the portal phase compared to non-contrast phase, yielded 90.9% sensitivity (60/66; 95% CI: 81.3–96.6), 94.3% specificity (66/70; 95% CI: 86.0–98.4) and an area under curve of 0.958 (95% CI: 0.919–0.996) for the diagnosis of NP versus IEP. Interobserver reproducibility for pancreas enhancement was good using Bland Altman plot and ICC was excellent for pancreatic gland analysis (ICC 0.978; 95% CI: 0.961–0.988) but poor or moderate (ICC ≤0.634) regarding peripancreatic fat necrosis.

Conclusion: By using a pancreas enhancement threshold value of 30 HU, CT is accurate and reproducible for the diagnosis of NP during the first week of the disease.

Abbreviations

AP	Acute pancreatitis
AUC	area under curve
C-	Unenhanced phase
C+	Enhaned phase
CI	Confidence interval
ICC	Intraclass correlation coefficient
IEP	Interstitial edematous pancreatitis
NP	Necrotic pancreatitis
RAC	Revised Atlanta Classification
ROC	Receiver operating characteristic
SIRS	Systemic inflammatory response syndrome
SD	Standard deviation

1. Introduction

Acute pancreatitis (AP) is a frequent and potentially life-threatening condition [1,2]. According to the 2012 Revised Atlanta Classification (RAC), AP can be classified into two distinct subtypes, which are necrotizing pancreatitis (NP) and interstitial edematous pancreatitis (IEP), based on the presence or absence of necrosis, respectively [3].

* Corresponding author.
E-mail address: jean-pierre.tasu@chu-poitiers.fr (J.P. Tasu).

https://doi.org/10.1016/j.diii.2021.12.003
2211-5684/

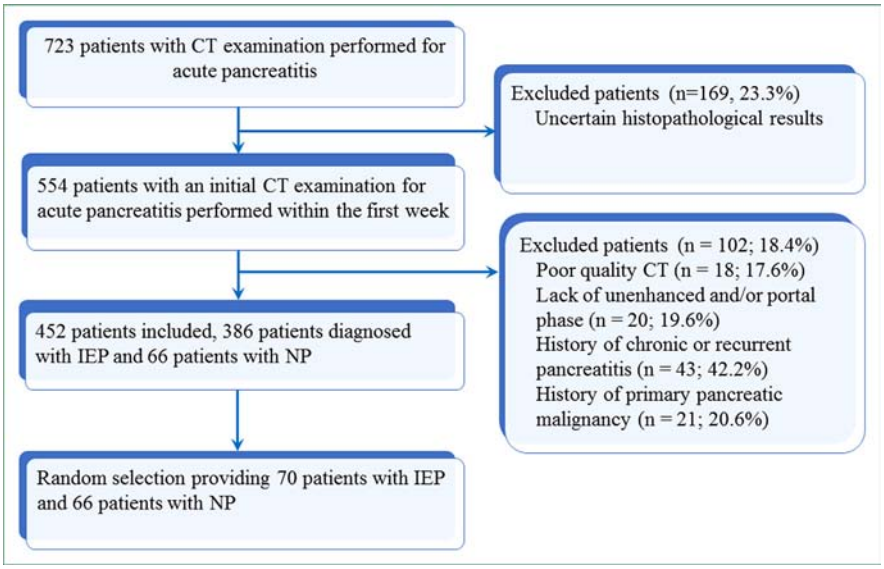

Fig. 1. Study flow chart. CT indicates computed tomography. NP indicates necrotic pancreatitis. IEP indicates interstitial edematous pancreatitis

IEP is more common and is associated with inflammation of the pancreas and/or the peripancreatic fat [4]; in this form, pancreas parenchyma shows enhancement on post-contrast computed tomography (CT) or magnetic resonance imaging examinations. NP represents only 15-20% of AP, involving either the pancreatic parenchyma and/or the peripancreatic tissues [5,6]. The diagnosis of pancreatic necrosis is made when a lack of glandular enhancement for pancreatic necrosis and/or a heterogeneous appearance of peri-pancreatic fat for extra-pancreatic necrosis are observed. When imaging is performed within the first few days following the onset of the disease, the diagnosis of pancreatic necrosis can be challenging because the parenchyma can present focal or global hypo-enhancing areas due to inflammation or the beginning of the necrosis process. In such situations, post-contrast CT examination performed 5–7 days later has been described as more accurate [3].

However, an international multicenter study demonstrated moderate agreement for the diagnosis of “parenchymal necrosis” (Kappa = 0.539) and “head necrosis” (Kappa=0.516) and fair agreement on the “type of pancreatitis” (Kappa = 0.370), and “extrapancreatic necrosis” (Kappa = 0.326) categories [7]. In a more recent single-center study, interobserver agreement was also moderate (Kappa = 0.45) for the detection of parenchymal necrosis during the first four weeks after the onset of symptoms and in categorization of peripancreatic collections (Kappa = 0.45) and did not improve with time to CT [8], a finding that was inconsistent with previous reports [9].

The point here is that the RAC definition of “glandular defect enhancement” has been based on visual reader evaluation alone, and is consequently insufficiently reliable. For this study, we made the hypothesis that inter-reader agreement could be improved by identifying an attenuation threshold value on CT to define necrosis during the acute phase of the disease.

The purpose of this study was to identify attenuation threshold value on CT that allowed discriminating between IEP and NP in patients with AP during the first week of the disease and evaluate interobserver reproducibility for the diagnosis of AP form.

2. Material and methods

This retrospective study was approved by our institutional review board (IRB # 12-2018) and requirements for informed consent of the patients was waived, in accordance with French legislation on retrospective studies using anonymized data.

2.1. Patients

The database of our Institution was queried to identify all patients with AP who underwent CT examination of the abdomen between March 2015 and December 2019. In accordance with the RAC [3], AP was defined as the presence of at least two of the following three features: abdominal pain consistent with AP disease, serum lipase at least 3-fold greater than the upper limit of normal, and/or imaging findings typical for AP. A total of 723 patients older than 18 years were initially retrieved. The first exclusion criterion was a delay between symptoms and CT examination of more than seven days (n = 169), and other exclusion criteria were poor-quality CT examinations (n = 18), lack of unenhanced and/or enhanced acquisition (n = 20), history of chronic or recurrent pancreatitis (n = 43), and history of primary pancreatic malignancy (n = 21). Out of the 452 patients included, patients with NP constituted the first group (n = 66), and a sample of IEP patients from the 386 remaining patients was randomly selected to constitute the second group. Fig. 1 shows the patient flow chart.

From the clinical discharge report, several parameters were recorded including sex, age, admission date, time from symptom to CT, presence, or lack of systemic inflammatory response syndrome (SIRS), etiology, organ failure (persistent and transient, in line with the RAC), presence and type of early and late (after one week according to RAC) complications and in-hospital mortality.

2.2. CT imaging technique

All abdominal CT examinations were performed with a single device (Aquilion® 64, Canon Medical Systems). All patients were examined in supine position. Image acquisition was performed in craniocaudal direction during breath-hold. The CT protocol included an abdominal unenhanced phase acquisition (C-) and at least one portal venous phase acquisition (C+) obtained 70 s after the beginning of the intravenous administration of contrast material (Iomeprol or Iomeron® 350, Bracco Imaging; Iobitridol, Xenetix® 350, Guerbet; Iohexol, Omnipaque® 350, GE Healthcare). The contrast mateiral was injected at a dose of 0.5 mg of iodine per kilogram of body weight and at a flow rate of 2.5–4 mL/s through a superficial vein of the

forearm. The CT settings used were: tube voltage of 100-120 Kv, mAs automatically modulated in z direction, 0.5 s rotation time, 1.4 pitch, 512 × 512 matrix and 0.5 mm collimation. All images were reconstructed with 2.0 mm section collimation in a 0.5 mm increment.

2.3. Reference diagnosis

Final clinical discharge report was used as reference for the diagnosis of AP category according to a multicriteria definition. AP associated with organ failure lasting more than 48 hours after onset of the disease and or one or more complications such as walled-off necrosis, pseudoaneurysm, vascular thrombosis and/or digestive fistula were considered in favor of NP. A lack of early or late complications except for pseudocyst, and/or CT performed seven days after the onset of the disease, demonstrating normal, diffuse, or localized enlargement of the pancreatic parenchyma with or without fluid collections lacking solid components, was considered in favor of IEP.

Infected collection suggesting NP was not sufficient for the diagnosis of AP category. Clinical and CT follow-ups were finally used to establish the final diagnosis of AP category.

2.4. Parameters and image analysis

One abdominal radiologist, reader 1 (R. L.G.) with five years of experience, reviewed each CT examination on a dedicated picture archiving and communication system unit (McKesson Radiology Station 11; McKesson Medical Imaging Group). Axial, coronal, and sagittal images could be used by the reader. The reader knew that the patients had AP but was unaware of other clinical data, including AP category. The CT images were analyzed for the presence of the following signs: criteria to assess mCTSI [9] (intrinsic pancreatic abnormalities with or without inflammatory changes in peri-pancreatic fat, pancreatic or peripancreatic fluid collection or peripancreatic fat necrosis, level of pancreatic necrosis ± 30% of total surface portal, extrapancreatic complications), splenic or mesenteric venous thrombosis. The reader had to manually place six regions of interest (ROI), on C- and C+ images, three within the pancreas, on the head, body and tail parts (further referred to as ROI1, ROI2, ROI3 respectively), and three in the corresponding anterior abdominal fat near the pancreas ROI (further referred to as ROI4, ROI5 and ROI6 respectively). ROIs were round and had a surface of at least 60 mm^2. ROIs were placed at the center of the pancreatic parenchyma in order to avoid partial volume bias, calcifications, vessels, necrotic collections, and pancreatic cysts, in an area where the enhancement seemed to be the weakest on portal phase. For peripancreatic fat, ROIs were placed in the peripancreatic area as close as possible to the corresponding pancreas ROI. One additional ROI (further referred to as ROI7) was placed on portal vein on C- (further referred to as $ROI7_{C-}$) and C+ (further referred to as $ROI7_{C+}$) images. Mean attenuation values in Hounsfield unit (HU) for each of the 14 ROIs per patient were used for analysis. Fig. 2 illustrates the placement of ROIs.

In each location, the difference in attenuation values of ROIs between before and after contrast enhancement during the portal phase for each location was computed. Because decreased enhancement of the pancreatic gland may be heterogenous, minimum enhancement value (ROI_{C+} - ROI_{C-}) was studied specifically among the three areas of pancreatic gland measures to consider the possible geographic variation of this parameter.

To take into account a possible impact of the quality of contrast injection and in accordance with a previous report [10], enhancement value was weighted by portal vein attenuation according to the ratio Rx: [($ROIx_{C+}$ - $ROIx_{C-}$)-($ROI7_{C+}$-$ROI7_{C-}$)]/($ROI7_{C+}$-$ROI7_{C-}$), and the minimum value of this ratio, the R index, was retained from the first 3 glandular ROIs.

2.5. Reproducibility study

In order to evaluate reproducibility, repeated measures were performed on 30 randomly selected patients by two other readers,

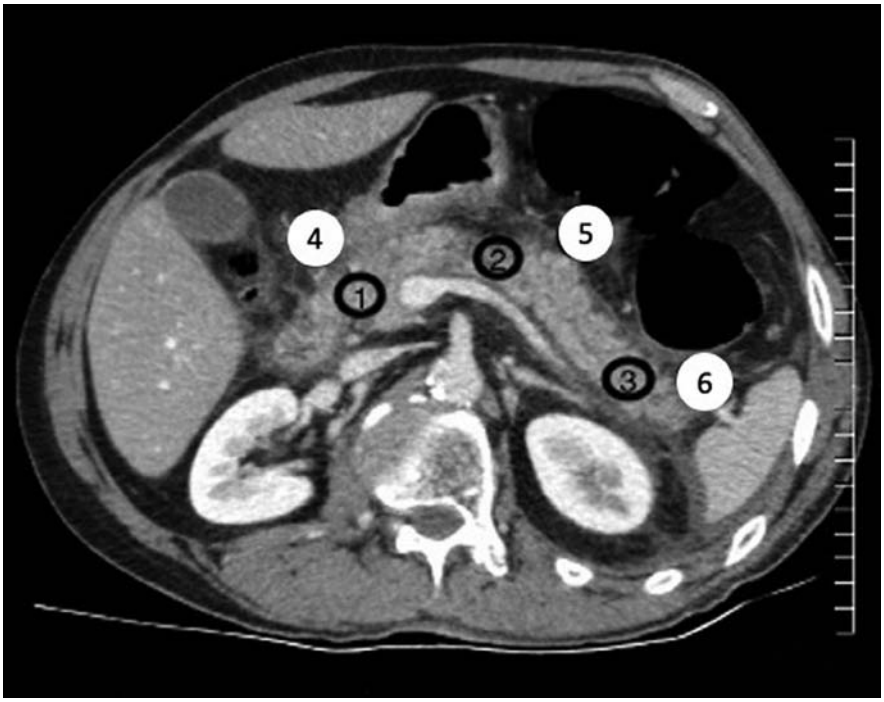

Fig. 2. 54-year-old woman with acute pancreatitis of biliary origin. Six regions of interest (ROI) are placed. Three ROIs are placed on the head, body and tail (ROI1, ROI2, ROI3 respectively) and three ROIs in the corresponding anterior abdominal fat near the pancreas (ROI4, ROI5 and ROI6 respectively). Two additional ROIs were placed on the portal trunk (not shown).

reader 2 (J.-P. T.) with 25 years of experience and reader 3 (I. B.R.), with six years of experience in abdominal imaging.

2.6. Statistical analysis

Quantitative variables were expressed as mean ± standard deviations (SD) and ranges, and qualitative variables as raw numbers, proportions and percentages. Mann-Whitney nonparametric test was used to compare attenuation data between AP categories. Threshold attenuations for the diagnosis of AP types were evaluated in terms of sensitivity and specificity with their corresponding 95% confidence intervals (CI). The discriminatory performance of pancreas enhancement was evaluated using a receiver operating characteristics (ROC) analysis with a calculation of area under the curve (AUC) as an overall accuracy estimate. Cross-validation (leave-one-out) was applied to obtain generalizable estimates of AUC and their 95%CI. An optimal cutoff was determined from the ROC curve using the Youden J index (Se + Sp - 1).

Interobserver agreement was estimated by the intraclass correlation coefficient (ICC) with 95% confidence limits obtained from a two-way random effect mixed model of analysis of variance [11], with ICC <0.5 indicating poor reliability, between 0.5 and 0.75 moderate, between 0.75 and 0.9 good, and ICC >0.9 indicating excellent reliability. Bland Altman plots were used to estimate reproducibility between pairs of observers with quantification of bias and 95% limits of agreement. Statistical significance was set at $P < 0.05$ (two-sided). Statistical analyses were performed with SAS version 9.4 (SAS Inc) and GraphPad Prism version 7.00 for Windows (GraphPad Software).

3. Results

3.1. Population characteristics

During the study period, 136 patients were evaluated; 66 patients (48.5%) had NP (46 men, 20 women; mean age, 55 ± 17 [SD] years; age range: 20–89 years) and 70 patients (51.5%) had IEP (39 men, 31 women; mean age, 54 ± 18 [SD] years; age range 21–87 years). Among patients with NP, there were 6 patients (9%) with peripancreatic necrosis and 60 patients (91%) with peripancreatic and pancreatic necrosis according to the RAC. Table 1 indicates the main characteristics of the two groups.

In patients with NP, the most common late complication was walled-off necrosis (33/66; 50%), followed by pancreatic necrosis infection (20/66; 30%), digestive fistula (9/66; 13%) and pseudoaneurysms/arterial erosion (5/66; 8%). Organ failure over 48 hours was observed in 5/66 patients (8%) and was the most common acute complication. Modified CTSI (mCTSI) score was 8.27 ± 1.26 (SD) (range 6–10) for patients with NP and 2.94 ± 2.20 (SD) (range: 0–8) for patients with IEP. Delay between symptoms and CT examination was 3.59 ± 1.68 (SD) days (range: 2–8 day) for patients with NP and 4.13 ± 1.42 (SD) days for patients with IEP (range: 2–7 day) (Table 1).

Table 1
Characteristics and complications in 136 patients with acute pancreatitis

Variables	Necrotizing AP (n = 66)	Interstitial edematous AP (n = 70)	*P*
Sex			0.110
Male	46 (70%)	39 (56%)	
Female	20 (30%)	31 (44%)	
Age (year)	55 ± 17 [20–89]	54 ± 18 [21–87]	0.900
Cause of AP			0.084
Biliary	20 (30%)	33 (47%)	
Alcoholic	25 (38%)	24 (34%)	
Other	21 (32%)	13 (19%)	
Complications			
Organ failure > 48 hours	34 (52%)	0 (0%)	<0.001
Renal failure	17 (26%)	0 (0%)	<0.001
Respiratory failure	12 (18%)	0 (0%)	<0.001
Shock	7 (11%)	0 (0%)	0.005
Arterial erosion/ aneurysm	5 (8%)	0 (0%)	0.025
Infected pancreatic necrosis	20 (30%)	0 (0%)	<0.001
Digestive fistula	9 (14%)	0 (0%)	0.001
SIRS	33 (50%)	0 (0%)	<0.001
Organized necrosis	25 (38%)	0 (0%)	<0.001
Severity (Atlanta)			<0.001
Mild	0 (0%)	57 (81%)	
Moderately severe	30 (46%)	13 (19%)	
Severe	35 (54%)	0 (0%)	
Mortality	6 (9%)	0 (0%)	0.012
Days from symptom to CT examination	3.59 ± 1.68 [2–8]	4.13 ± 1.42 [2-7]	0.018
mCTSI Score	8.27 ± 1.26 [6–10]	2.94 ± 2.20 [0–8]	<0.001
Lipasemia (IU/L)	2235 ± 3165 [30 –18240]	1058 ± 1070 [158 –4940]	0.015
SIRS	55 (85%)	25 (37%)	<0.001

Qualitative variables are expressed as raw numbers followed by percentages in parentheses. Quantitative variables are expressed as means ± standard deviations followed by ranges in brackets.
AP = Acute pancreatitis; mCTSI = Modified CT score index; SIRS = Systemic inflammatory response syndrome; IU = International unit.

3.2. CT image analysis

The results of comparisons of attenuation values and enhancement of pancreatic gland and peripancreatic fat between NP and IEP are presented in Table 2. Enhancement were different between the two AP categories (P <0.001) in the three ROIs placed on the pancreatic gland; AUCs were 0.859, 0.862 and 0.866 for RO1, ROI2 and ROI3 respectively. Considering the minimal ROI enhancement value in pancreatic gland, AUC was 0.958 (95% CI: 0.919–0.996); a threshold value of 30 HU was associated with 90.9% sensitivity (60/66; 95% CI: 81.3–96.9) and 94.3% specificity (66/70; 95% CI: 86.0–98.4) for the diagnosis of NP versus IEP (Fig. 3). No CT attenuation threshold value was found to diagnose peripancreatic fat necrosis.

Regarding the R index, AUC was 0.953 (95% CI: 0.915–0.992) and with a threshold of -0.7, sensitivity was 90.9% (60/66; 95% CI 81.3 –96.9) and specificity 94.3% (66/70; 95% CI 85.8–98.4). Stratified analysis relating to delay between symptom onset and CT examination demonstrated no significant differences between ROC curves of minimal ROI enhancement (P = 0.50), before (AUC = 0.963; 95% CI: 0.911–0.999) and after three days (AUC = 0.931; 95% CI: 0.851 –0.999).

3.3. Reproducibility

Among the 30 randomly selected patients, 11 patients had NP and 19 had IEP. Results of Bland Altman plots analysis are reported in Table 3 and Fig. 4. Results of ICC analysis are reported in Table 3. ICC was > 0.9 for all pancreatic ROIs, corresponding to excellent interobserver agreement, but ICC was ≤ 0.634 for peripancreatic fat (Table 3). ICC was 0.978 (95% CI: 0.961–0.988) for the minimum enhancement value and 0.964 (95% CI: 0.935–0.981) for the R index (Table 3).

4. Discussion

A CT-based subjective diagnosis of early AP category based on pancreatic parenchyma enhancement modifications is sometimes challenging in daily clinical routine. Our results show that a CT threshold of 30 HU for pancreatic enhancement is accurate in the diagnosis of pancreatic necrosis and associated with excellent interobserver reproducibility and not influenced by enhancement of the

Table 2
Attenuation (enhancement, minimal pancreatic gland enhancement value) and R index in 66 patients with necrotizing acute pancreatitis and 70 patients with interstitial edematous acute pancreatitis

		Necrotizing AP (n = 66)	Interstitial edematous AP (n = 70)	*P*
Pancreatic gland	ROI1 C-	32.5 ± 9.8	39.4 ± 10.7	< 0.001
	ROI1 C+	61.1 ± 25.7	97.9 ± 20.2	< 0.001
	ROI1 DC	28.6 ± 20.8	58.4 ±15.3	< 0.001
	ROI2 C-	32.4 ± 10.2	38.8 ± 9.2	< 0.001
	ROI2 C+	59.0 ± 24.4	97.0 ± 20.1	< 0.001
	ROI2 DC	26.6 ± 22.1	58.2 ± 15.5	< 0.001
	ROI3 C-	32.7 ± 11.8	39.6 ± 9.5	< 0.001
	ROI3 C+	58.1 ± 26.3	98.0 ± 18.1	< 0.001
	ROI3 DC	25.5 ± 23.1	58.4 ± 15.3	< 0.001
Peripancreatic fat	ROI4 C-	-47.4 ± 35.3	-62.8 ± 46.0	0.010
	ROI4 C+	-31.7 ± 38.3	-52.3 ± 48.2	0.010
	ROI4 DC	15.7 ± 20.1	10.5 ± 18.2	0.040
	ROI5 C-	-55.6 ± 33.4	-64.44 ± 46.0	0.070
	ROI5 C+	-40.0 ± 43.5	-49.81 ± 46.9	0.260
	ROI5 DC	15.6 ± 20.8	14.6 ± 19.7	0.88
	ROI6 C-	-49.3 ± 32.6	-66.5 ± 44.2	0.01
	ROI6 C+	-34.1 ± 36.9	-52.9 ± 45.2	0.01
	ROI6 DC	15.3 ± 18.3	13.6 ± 20.4	0.32
Portal vein	ROI7 C-	39.4 ± 7.8	41.7 ± 4.9	0.02
	ROI7 C+	149.3 ± 23.8	160.9 ± 22.9	< 0.001
	ROI7 DC	110 ± 23.8	119.3 ± 22.2	0.01
ROI 1,2,3	Min DC	10.9 ±14.3	51.6 ± 14.3	< 0.001
	R	0.39 ± 0.17	0.61 ± 0.08	< 0.001

Variables are expressed as means ± standard deviations in Hounsfield units. Measurements were performed before (C-) and after injection (C+); DC enhancement (formula: C+ minus C-); Min DC indicates minimum enhancement value in pancreatic gland; R indicates minimum enhancement ratio in pancreatic gland weighted by portal vein enhancement.
AP = Acute pancreatitis; ROI = Region of interest.

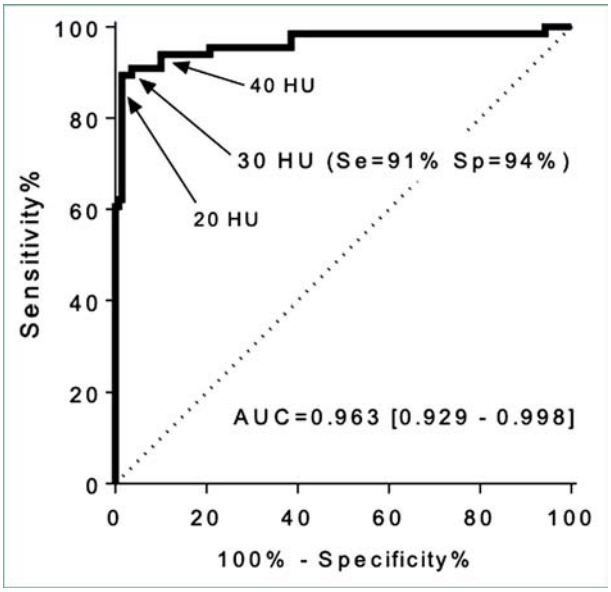

Fig. 3. Graph shows ROC curve of minimal pancreatic gland enhancement for the discrimination between necrotizing and interstitial edematous acute pancreatitis.

portal vein. According to Balthazar et al. [12], an ideal AP detection tool should have high sensitivity, be able to depict necrosis early (ideally within 48 hours), be performed rapidly, be available in most hospitals, be relatively inexpensive, and be objective and not observer-dependent. With a CT density threshold, all these criteria are met, thereby reinforcing the role of CT imaging in the early phase of AP.

While the RAC defines NP as "glandular defect enhancement", this criterion remains subjective, linked to visual analysis, and has been shown to be poorly reproducible [7, 8]. A precise attenuation threshold has previously been validated in many fields of radiology and helps improve reproducibility; this can be illustrated by the Bosniak's classification used for kidney cysts [13]. For renal cysts, a threshold of 20 HU is commonly admitted, while a threshold of >20 HU increases the specificity of identifying a mass as solid, but at the penalty of a lower sensitivity. For the pancreas, our study is to our knowledge the first to determine a threshold for pancreatic enhancement. Preconstrast pancreatic CT attenuations of 40–50 HU on unenhanced CT images are expected to increase to 100–150 HU after intravenous administration of contrast material. Balthazar et al. suggested that a lack of contrast enhancement or minimal contrast enhancement of less than 30 HU of the pancreas indicated decreased ischemia and was associated with the development of necrosis [12]. This statement was likely based on his personal experience, rather than on a dedicated study. Only one study has focused on "fulminant pancreatitis", showing decreased enhancement (from 0 to 15 HU; $P < 0.001$) after contrast injection compared to less severe forms that were associated with an enhancement between 30 and 40 HU [14]. However, this study included only 28 patients and these results may not be reproducible with recent CT technology, factors limiting the power of these results [14]. In the same idea and more recently, Liu et al. showed than mean pancreatic CT density based on CT can provide early prediction of persistent organ failure or infected pancreatic necrosis [15].

The explanation for lack of enhancement in NP is well-known. In IEP, the pancreatic capillary network is not affected, presenting vasodilation associated with persistent post-contrast enhancement. In NP, the pancreatic capillary network is digested by the pancreatic enzymes, leading to areas of decreased or absent enhancement [16].

Several factors and potential pitfalls should be kept in mind regarding pancreas attenuation measurement: First, pancreatic enhancement can be substantially decreased when fatty infiltration is present [17]. Second, it has been reported that a slight variation in the enhancement values of the head, body, and tail of the pancreas is sometimes observed in healthy individuals [18]. Impact of localized or diffuse change in the texture of the gland must be sought out. Third, presumed pancreatic ischemia manifesting as areas of decreased attenuation on the initial CT examination could be

Table 3
Reproducibility analysis among three observers in 30 randomly selected patients for ROI measurements before and after injection, enhancement, minimum enhancement and R index values.

		Reader 1	Reader 2	Reader 3	Reader 3 *vs.* Reader 1		Reader 3 *vs.* Reader 2		Reliability (3 observers)
					Bias	*P*	Bias	*P*	ICC (95% CI)
Pancreatic gland	ROI1 C-	38.2 ± 11.0	38.9 ± 10.8	38.6 ± 10.3	0.37 ± 4.28	0.64	-0.33 ± 3.51	0.61	0.938 (0.889–0.966)
	ROI1 C+	92.9 ± 24.7	92.1 ± 24.4	92.3 ± 24.7	-0.60 ± 3.82	0.40	0.17 ± 3.26	0.78	0.987 (0.976–0.993)
	ROI1 DC	54.7 ± 18.9	53.2 ± 18.8	53.7 ± 20.0	-0.97 ± 5.51	0.34	0.50 ± 34.85	0.58	0.962 (0.931–0.979)
	ROI2 C-	38.3 ± 9.6	37.9 ± 9.5	38.2 ± 10.3	-0.10 ± 3.17	0.86	0.33 ± 2.75	0.51	0.954 (0.917–0.975)
	ROI2 C+	91.2 ± 26.1	90.4 ± 25.3	91.2± 25.9	-0.07 ± 3.85	0.93	0.80 ± 3.24	0.19	0.990 (0.982–0.995)
	ROI2 DC	52.9 ± 21.2	52.5 ± 19.6	53.0 ± 20.5	0.03 ± 4.79	0.97	0.47 ± 3.91	0.52	0.976 (0.957–0.987)
	ROI3 C-	39.8 ± 8.4	39.1 ± 8.4	39.8 ± 8.6	-0.03 ± 3.63	0.96	0.70 ± 3.11	0.23	0.915 (0.850–0.953)
	ROI3 C+	92.1 ± 23.9	91.3 ± 23.1	91.5± 23.9	-0.53 ± 3.31	0.38	0.20 ± 4.17	0.79	0.988 (0.978–0.994)
	ROI3 DC	52.3 ± 22.2	52.3 ± 20.5	51.8 ±22.9	-0.50 ± 5.32	0.61	-0.50 ± 5.49	0.62	0.972 (0.949–0.985)
Peripancreatic fat	ROI4 C-	-69.3 ± 34.0	-78.7 ± 22.6	-66.0 ± 35.1	3.33 ± 37.69	0.63	12.70 ± 22.51	0.01	0.487 (0.291–0.687)
	ROI4 C+	-51.9 ± 39.5	-64.1 ± 28.5	-47.1 ± 38.4	4.83 ± 46.22	0.57	17.07 ± 22.63	<0.001	0.436 (0.241–0.652)
	ROI4 DC	17.4 ± 27.2	14.6 ± 9.6	18.9 ± 19.3	1.50 ± 32.94	0.80	4.37 ± 18.87	0.22	0.091 (0.007–0.594)
	ROI5 C-	-70.0 ± 35.3	-78.6 ± 29.2	-67.0 ± 33.2	3.03 ± 31.20	0.60	11.60 ± 28.88	0.04	0.634 (0.453–0.784)
	ROI5 C+	-64.2 ± 35.8	-67.5 ± 32.2	-44.5 ± 47.1	19.73 ± 43.47	0.02	22.97 ± 41.57	0.01	0.479 (0.283–0.681)
	ROI5 DC	5.8 ±24.4	11.1 ± 9.0	22.5 ± 23.4	16.70 ± 36.61	0.02	11.37 ± 23.75	0.01	0.000
	ROI6 C-	-70.8 ± 34.7	-81.7 ± 19.8	-68.7 ± 33.5	2.03 ± 30.15	0.71	12.93 ± 23.99	0.01	0.528 (0.333–0.714)
	ROI6 C+	-55.5 ± 45.6	-71.5 ± 25.0	-47.7 ± 43.9	7.83 ± 47.65	0.38	23.80 ± 36.22	<0.001	0.336 (0.153–0.586)
	ROI6 DC	15.2 ± 36.5	10.2 ± 9.4	21.0 ± 20.9	5.80 ± 40.44	0.44	10.87 ± 21.94	0.01	0.021 (0.000–0.998)
Portal vein	ROI7 C-	41.2 ± 5.6	40.3 ±4.4	41.3 ± 5.1	0.07 ± 4.40	0.93	0.93 ± 3.01	0.10	0.698 (0.532–0.824)
	ROI7 C+	163.9 ± 26.1	163.8 ± 26.5	164.3 ± 26.3	0.33 ± 3.21	0.57	0.50 ± 3.22	0.40	0.993 (0.986–0.996)
	ROI7 DC	122.7 ± 24.1	123.4 ± 25.2	123.0 ± 25.5	0.27 ± 5.64	0.80	-0.43 ± 4.12	0.57	0.979 (0.961–0.989)
ROI 1, 2, 3	Min DC	46.6 ± 21.5	46.1 ± 20.6	45.8 ± 22.8	-0.27 ± 4.73	0.98	-0.77 ± 4.32	0.98	0.978 (0.961–0.988)
	R index	-0.62 ± 0.17	-0.62 ± 0.16	-0.62 ± 0.17	-0.004 ± 0.041	0.57	0.002 ± 0.040	0.78	0.964 (0.935–0.981)

Bias is expressed as mean ± standard deviation of differences between paired observations. DC enhancement (formula: C+ minus C-); Min DC indicates minimum enhancement value in pancreatic gland; CI = Confidence interval; ICC = Intraclass correlation coefficient; ROI = Region of interest.

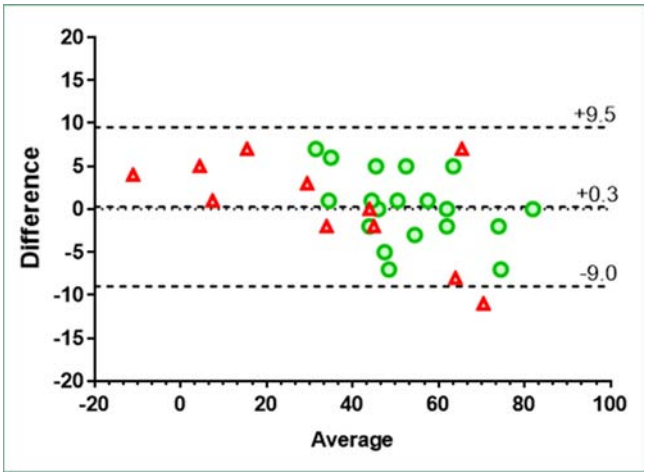

Fig. 4. Graph shows Bland Altman plots for inter-observer reproducibility for minimal pancreatic gland CT enhancement for two observers. Dotted lines represent mean bias and 95% limits of agreement. Red triangles represent patients with necrotic pancreatitis (n = 11) and green circles patients with interstitial edematous pancreatitis (n = 19).

reversible; all these points are subjected to speculation and require further study [19].

Dynamic CT with perfusion imaging allows assessment of pancreas perfusion by evaluating the degree of ischemic change associated with AP severity [20]. One study revealed that pancreatic blood flow, blood volume and mean transit time were significantly lower in patients who developed severe AP in the presence of pancreatic and/or peripancreatic necrosis [21]. However, there was a large overlap in all these parameters between mild and severe AP forms. In addition, the rate of failed examination may reach up to 23% [20], and the method requires a breath-hold of 40 s, which might be difficult to achieve in acutely ill patients.

Dual-energy CT technique is a promising technique that has several applications in the abdomen [22, 23]. This technique was recently evaluated for the early diagnosis of acute pancreatitis [24]. Iodine attenuation parameter was associated with better performance (AUC = 0.855) than attenuation value measurement (AUC = 0.835) and visual analysis (AUC = 0.797) in the diagnosis of AP, iodine attenuation being lower in AP compared to normal pancreas. The authors explained this apparent discrepancy by increased capillary permeability in pancreatitis with subsequent fluid loss, to a greater extent than in normal pancreas [24]. Despite these interesting results, experience with the iodine quantification technique in pancreas imaging remains scarce and material decomposition analysis has yet to be investigated as a means of diagnosing pancreatitis forms. Given its high tissue contrast, the place of magnetic resonance imaging should be considered as an alternative imaging method. Further studies are nonetheless required.

In our study, we did not find a CT attenuation threshold value to diagnose peripancreatic fat necrosis. This result could be explained by poor vascularization of fat. However, dual-energy CT seems to discriminate between different fat contents at low energy levels after contrast enhancement [25]. These promising results should warrant further studies.

Our study has some limitations. The results of the diagnostic accuracy analysis should be considered with caution given our retrospective study design, which can be associated with potential selection bias. Although we adopted randomized patient selection to mitigate this limitation, a prospective study is required to validate our initial results. Another limitation is that we investigated portal-phase images. The imaging standard for the pancreas is commonly the pancreatic phase, which occurs earlier [26]. However, it is commonly admitted that in AP, the portal phase is used to evaluate pancreatic parenchyma enhancement [27]. In addition, the use of a fixed time interval for the portal phase may have influenced our results, given that this technique does not take into account cardiac functions or quality of contrast material administration. However, we have shown that inclusion of portal enhancement does not change diagnostic accuracy. The absence of histological confirmation could be an issue; the diagnosis of AP category was therefore performed during patient follow-up, and we cannot rule out the possibility that some mild NPs were incorrectly classified because of the lack of complications. Indeed, the definition used here to define NP corresponds more to severe AP according to RAC

criteria [3]. Consequently, the threshold proposed here could correctly classify non severe forms as opposed to severe forms more than IEP and NP. Finally, we did not evaluate the capabilities of more refined quantitative imaging features to discriminate between NP and IEP [28–30]

In conclusion, this study shows that pancreas enhancement on post contrast CT images less than 30 UH during the portal phase is an accurate and reproducible threshold to diagnose NP. However, we failed to identify a CT attenuation threshold value to diagnose peripancreatic fat necrosis.

Human rights

The authors declare that the work described has been carried out in accordance with the Declaration of Helsinki of the World Medical Association revised in 2013 for experiments involving humans.

Informed consent and patient details

The authors declare that this report does not contain any personal information that could lead to the identification.

Funding

This work did not receive any grant from funding agencies in the public, commercial, or not-for-profit sectors.

Author contributions

All authors attest that they meet the current International Committee of Medical Journal Editors (ICMJE) criteria for Authorship.

Disclosure of interest

The authors declare that they have no competing interest.

References

[1] Frossard JL, Steer ML, Pastor CM. Acute pancreatitis. Lancet 2008;371:143–52.
[2] Zhang C, Li A, Luo T, Li J, Liu D, Cao F, et al. Strategy and management of severe hemorrhage complicating pancreatitis and post-pancreatectomy. Diagn Interv Radiol 2019;25:81–9.
[3] Banks PA, Bollen TL, Dervenis C, Gooszen HG, Johnson CD, Sarr MG, et al. Classification of acute pancreatitis–2012: revision of the Atlanta classification and definitions by international consensus. Gut 2013;62:102–11.
[4] Bhatia M, Wong FL, Cao Y, Lau HY, Huang J, Puneet P, et al. Pathophysiology of acute pancreatitis. Pancreatology 2005;5:132–44.
[5] Bakker OJ, van Santvoort H, Besselink MG, Boermeester MA, van Eijck C, Dejong K, et al. Extrapancreatic necrosis without pancreatic parenchymal necrosis: a separate entity in necrotising pancreatitis? Gut 2013;62:1475–80.
[6] Sharma V, Rana SS, Bhasin DK. Extra-pancreatic necrosis alone: contours of an emerging entity. J Gastroenterol Hepatol 2016;31:1414–21.
[7] Sternby H, Verdonk RC, Aguilar G, Dimova A, Ignatavicius P, Ilzarbe L, et al. Significant inter-observer variation in the diagnosis of extrapancreatic necrosis and type of pancreatic collections in acute pancreatitis: an international multicenter evaluation of the revised Atlanta classification. Pancreatology 2016;16:791–7.
[8] Badat N, Millet I, Corno L, Khaled W, Boulay-Coletta I, Zins M. Revised Atlanta classification for CT pancreatic and peripancreatic collections in the first month of acute pancreatitis: interobserver agreement. Eur Radiol 2019;29:2302–10.
[9] Mortele KJ, Wiesner W, Intriere L, Shankar S, Zou KH, Kalantari BN, et al. A modified CT severity index for evaluating acute pancreatitis: improved correlation with patient outcome. AJR Am J Roentgenol 2004;183:1261–5.
[10] Gulpinar B, Peker E, Kul M, Elhan AH, Haliloglu N. Liver metastases of neuroendocrine tumors: is it possible to diagnose different histologic subtypes depending on multiphasic CT features? Abdom Radiol 2019;44:2147–55.
[11] Benchoufi M, Matzner-Lober E, Molinari N, Jannot AS, Soyer P. Interobserver agreement issues in radiology. Diagn Interv Imaging 2020;101:639–41.
[12] Balthazar EJ. Acute pancreatitis: assessment of severity with clinical and CT evaluation. Radiology 2002;223:603–13.
[13] Bosniak MA. The current radiological approach to renal cysts. Radiology 1986;158:1–10.
[14] Kivisaari L, Somer K, Standertskjold-Nordenstam CG, Schroder T, Kivilaakso E, Lempinen M. Early detection of acute fulminant pancreatitis by contrast-enhanced computed tomography. Scand J Gastroenterol 1983;18:39–41.
[15] Liu N, He J, Hu X, Xu SF, Su W, Luo JF, et al. Acute necrotising pancreatitis: measurements of necrosis volume and mean CT attenuation help early prediction of organ failure and need for intervention. Eur Radiol 2021;31:7705–14.
[16] Block S, Maier W, Bittner R, Buchler M, Malfertheiner P, Beger HG. Identification of pancreas necrosis in severe acute pancreatitis: imaging procedures versus clinical staging. Gut 1986;27:1035–42.
[17] Garcia TS, Rech TH, Leitao CB. Pancreatic size and fat content in diabetes: a systematic review and meta-analysis of imaging studies. PLoS One 2017;12:e0180911.
[18] Balthazar EJ, Robinson DL, Megibow AJ, Ranson JH. Acute pancreatitis: value of CT in establishing prognosis. Radiology 1990;174:331–6.
[19] Aho HJ, Nevalainen TJ, Aho AJ. Experimental pancreatitis in the rat. Development of pancreatic necrosis, ischemia and edema after intraductal sodium taurocholate injection. Eur Surg Res 1983;15:28–36.
[20] Bize PE, Platon A, Becker CD, Poletti PA. Perfusion measurement in acute pancreatitis using dynamic perfusion MDCT. AJR Am J Roentgenol 2006;186:114–8.
[21] Pienkowska J, Gwozdziewicz K, Skrobisz-Balandowska K, Marek I, Kostro J, Szurowska E, et al. Perfusion-CT: can we predict acute pancreatitis outcome within the first 24 hours from the onset of symptoms? PLoS One 2016;11:e0146965.
[22] Dabli D, Frandon J, Belaouni A, Akessoul P, Addala T, Berny L, et al. Optimization of image quality and accuracy of low iodine concentration quantification as function of dose level and reconstruction algorithm for abdominal imaging using dual-source CT: a phantom study. Diagn Interv Imaging 2021. doi: 10.1016/j.diii.2021.08.004.
[23] Greffier J, Dabli D, Hamard A, Akessoul P, Belaouni A, Beregi JP, et al. Impact of dose reduction and the use of an advanced model-based iterative reconstruction algorithm on spectral performance of a dual-source CT system: A task-based image quality assessment. Diagn Interv Imaging 2021;102:405–12.
[24] Martin SS, Trapp F, Wichmann JL, Albrecht MH, Lenga L, Durden J, et al. Dual-energy CT in early acute pancreatitis: improved detection using iodine quantification. Eur Radiol 2019;29:2226–32.
[25] Rodriguez-Granillo GA, Capunay C, Deviggiano A, De Zan M, Carrascosa P. Regional differences of fat depot attenuation using non-contrast, contrast-enhanced, and delayed-enhanced cardiac CT. Acta Radiol 2019;60:459–67.
[26] Fletcher JG, Wiersema MJ, Farrell MA, Fidler JL, Burgart LJ, Koyama T, et al. Pancreatic malignancy: value of arterial, pancreatic, and hepatic phase imaging with multi-detector row CT. Radiology 2003;229:81–90.
[27] Noda Y, Goshima S, Fujimoto K, Kawada H, Kawai N, Tanahashi Y, et al. Utility of the portal venous phase for diagnosing pancreatic necrosis in acute pancreatitis using the CT severity index. Abdom Radiol 2018;43:3035–42.
[28] Park S, Chu LC, Hruban RH, Vogelstein B, Kinzler KW, Yuille AL, et al. Differentiating autoimmune pancreatitis from pancreatic ductal adenocarcinoma with CT radiomics features. Diagn Interv Imaging 2020;101:555–64.
[29] Barat M, Chassagnon G, Dohan A, Gaujoux S, Coriat R, Hoeffel C, et al. Artificial intelligence: a critical review of current applications in pancreatic imaging. Jpn J Radiol 2021;39:514–23.
[30] Park S, Chu LC, Fishman EK, Yuille AL, Vogelstein B, Kinzler KW, et al. Annotated normal CT data of the abdomen for deep learning: Challenges and strategies for implementation. Diagn Interv Imaging 2020;101:35–44.